



HAL
open science

MRI diagnosis of saccular hydrops: Comparison of heavily-T2 FIESTA-C and 3D-FLAIR sequences with delayed acquisition

Michael Eliezer, Guillaume Poillon, Julien Horion, Phillipe Lelion, Emmanuel Gerardin, Nicolas Magne, André Gillibert, Arnaud Attyé

► To cite this version:

Michael Eliezer, Guillaume Poillon, Julien Horion, Phillipe Lelion, Emmanuel Gerardin, et al.. MRI diagnosis of saccular hydrops: Comparison of heavily-T2 FIESTA-C and 3D-FLAIR sequences with delayed acquisition. *Journal de Neuroradiologie / Journal of Neuroradiology*, 2021, 48 (6), pp.446-452. 10.1016/j.neurad.2019.04.005 . hal-04841547

HAL Id: hal-04841547

<https://hal.science/hal-04841547v1>

Submitted on 19 Dec 2024

HAL is a multi-disciplinary open access archive for the deposit and dissemination of scientific research documents, whether they are published or not. The documents may come from teaching and research institutions in France or abroad, or from public or private research centers.

L'archive ouverte pluridisciplinaire **HAL**, est destinée au dépôt et à la diffusion de documents scientifiques de niveau recherche, publiés ou non, émanant des établissements d'enseignement et de recherche français ou étrangers, des laboratoires publics ou privés.



Distributed under a Creative Commons Attribution - NonCommercial 4.0 International License

MRI diagnosis of saccular hydrops: comparison of heavily-T2 FIESTA-C and 3D-FLAIR sequences with delayed acquisition

Original Research

Michael Eliezer, MD ¹ – Guillaume Poillon, MD ¹ – Julien Horion, MD ¹ –
Phillipe Lelion, MD ² – Emmanuel Gerardin, MD, PhD ¹ – Nicolas Magne, MD,
¹ – André Gillibert, MD ³ – Arnaud Attyé, MD ^{1,4}

1 Department of Neuroradiology and MRI, Rouen University Hospital, Rouen –
France

2 Department of Head and Neck Surgery, Rouen University Hospital, Rouen –
France

3 Department of Biostatistics, Rouen University Hospital, Rouen – France

4 Department of Neuroradiology and MRI, Grenoble Alpes University Hospital
– SFR RMN Neurosciences, Grenoble – France

Corresponding author

Michael ELIEZER

Neuroradiology and MRI Unit

Rouen University Hospital

76000 Rouen, France

Tel: +33 2 32 88 89 90

E-Mail: mcheliezer@gmail.com

Manuscript title:

MRI diagnosis of saccular hydrops: comparison of heavily-T2 FIESTA-C and 3D-FLAIR sequences with delayed acquisition

Manuscript type: Original research

ABSTRACT

PURPOSE:

Currently, 3D-FLAIR sequence performed 4 hours after the intravenous administration of a single dose of contrast media is the imaging technique of choice for the diagnosis of saccular hydrops (SH). Recently, the diagnosis of SH has also been reported with heavily-T2 weighted sequences.

MATERIALS AND METHODS:

In this retrospective imaging study, we performed 3D-FLAIR sequences 4 hours after contrast media administration and 3D FIESTA-C sequences before and 4 hours after contrast media administration in 30 patients with unilateral definite, probable or possible clinical diagnosis of Menière's disease (MD). Two radiologists, blinded to the clinical data, independently assessed the presence of saccular hydrops. Inter-reader agreement tests were performed.

RESULTS:

On delayed post-contrast 3D-FLAIR sequence, 15 patients out of 30 referred with a SH that was never seen on the contralateral asymptomatic side. The specificity and the sensitivity to detect MD side were 100% and 50% respectively. On non-enhanced 3D FIESTA-C sequence, 16 patients out of 30 (53%) referred with a saccular hydrops that was observed in 6 patients on the clinical asymptomatic ear. The specificity and the sensitivity to detect MD side were 80% and 33% respectively. On delayed 3D FIESTA-C sequence, 13 patients out of 30 (43%) referred with a saccular hydrops that was seen in 4 patients on the contralateral asymptomatic side. The specificity and the sensitivity to detect MD side were 83% and 27% respectively.

CONCLUSION:

Delayed post-contrast 3D-FLAIR is highly specific of MD symptoms while 3D FIESTA-C sequences are less sensitive and specific for the diagnosis of SH.

Keywords

Endolymphatic hydrops; Menière's disease; MRI

Introduction:

Since the first description by Altmann and Fowler, endolymphatic hydrops is considered to be related with Meniere's Disease (MD) ¹. The diagnosis of MD is based on clinical findings, however temporal bone MRI is always performed to exclude other pathologies mimicking MD, such as vestibular schwannoma, endolymphatic sac tumor or intracranial hypotension.

Currently, **delayed 3D-FLAIR sequence** is the imaging technique of choice for the diagnosis of endolymphatic hydrops ². Naganawa et al. provided a method to assess the endolymphatic space on MRI with 3D-FLAIR sequences delayed acquisition after the intravenous administration of gadolinium ³. The gadolinium crosses the blood-perilymph barrier progressively with a plateau between 4 and 6 hours ⁴. The perilymph appears as a high-signal while the endolymph remains with low-signal because gadolinium does not pass the blood-endolymph and the perilymph-endolymph barriers due to the presence of tight junctions ^{5,6}. Based on the fact that the saccule is mainly involved in MD pathophysiology owing to its high mechanical compliance ⁷, the diagnosis of saccular hydrops (SH) has been proposed using the SURI technique (saccular utricular ratio inversion) ^{8,9}. It has been demonstrated highly specific to MD and less dependent on the sequence parameter ¹⁰ but only in patients with at least 40 dB of hearing loss ¹¹.

Recently, the diagnosis of SH has been reported on two studies with routine non-enhanced 3D Heavily-T2 weighted sequences ^{12,13}. Heavily-T2 weighted sequences have allowed the diagnosis of EH based on the measure of the saccular height and width in a coronal plane in MD patients in comparison to a control group with healthy inner ears.

The aim of this study was to compare the diagnosis accuracy of saccular hydrops in MD patients, as measured with post-contrast 3D-FLAIR and 3D Heavily-T2 weighted sequences.

Methods:

Patients

This was a retrospective single center imaging study. Thirty patients having a unilateral definite, probable or possible clinical diagnosis of MD based on the AAO-HNS guidelines were recruited between December 2016 and October 2017¹⁴. The pure-tone average (PTA) hearing levels of bone conduction were calculated as the mean of the hearing levels measured at 500, 1000, 2000, and 4000 Hz. Patients' hearing was classified as mild (26-40 dB), moderate (41-60 dB), severe (61-80 dB) and profound (over 81 dB). Patients with a history of surgery or intratympanic therapy such as gentamicin were excluded based on the supplemental risk of post-treatment hearing loss.

The study protocol was approved by our institutional review board (IRB E2017-23).

Imaging

All patients had an MRI scan before and after the administration of a single intravenous dose of Gadobutrol, Gadovist® (Gd-BT-DO3A, 0.1 mmol/kg) that provide a high contrast¹⁵. Imaging examinations were carried out on a 3T

General Electric Discovery® MRI scanner with a surface coil (FLEX) providing high signal to noise ratio.

We performed 3D-FLAIR MRI sequence with the CUBE® technique 4 hours after contrast media administration, with the following parameters: TR: 8000ms, TE: 130ms, TI: 2059ms, 288x288, variable flip angle and isotropic voxel size of 1 mm for acquisition and 0.5 mm for reconstructions. We employed the ARC parallel imaging technique with an acceleration factor of 2, nex: 1, and a scan time of 7'30.

Since it was reported that 3D-FIESTA sequence is sensitive to gadolinium we performed this sequence before and 4 hours after contrast media administration to assess the endolymphatic space before and after the perilymphatic enhancement and to evaluate the reproducibility of this sequence ¹⁶. The parameters were: TR: 7 ms, TE: 2.8 ms, NEX: 1, matrix: 484x484, flip angle: 60°, bandwidth: 83.3 kHz, 0.3 mm slice thickness covering the labyrinth with a 20 cm field of view. We employed the ARC parallel imaging technique with an acceleration factor of 2 and a scan time of 4'40.

Both 3D-FLAIR and 3D-FIESTA-C sequences were performed in the plane of the lateral semicircular canal.

Analysis: saccular-based morphology grading

Images for each subject were evaluated independently by two radiologists (readers) who were blinded to the clinical data. The imaging data of ears were analyzed with Osirix MD®.

Using the 3D-FLAIR delayed post-contrast, we graded saccular hydrops using the SUR1 technique defined as the ratio between the area of the saccule and the area of the utricle, as evaluated in axial and sagittal slice on one reference image. Saccular hydrops was defined (Fig. 1) as when the saccule appeared equal or larger than the utricle, in both radiologists' qualitative evaluations⁸⁻¹¹. Using the 3D FIESTA-C sequence, we defined (Fig. 1) saccular hydrops, as previously reported by measuring the height and the width of the saccule in a coronal plane passing through the lateral and superior ampullas^{12,13}. The saccular height was measured vertically from the utricular macula to the inferior limit of the saccule appearing as a low-signal. The saccular width was measured horizontally at its largest from the medial bone to the vertical low-signal corresponding to the lateral saccular wall. We decided to base our measurement on the results of Venkatasamy et al since the image examination was realized on the same MRI machine and because the parameters of the 3D FIESTA-C were closely similar¹³. The height and the width were considered as pathological when superior or equal to 1.7 and 1.5 mm respectively.

Statistical analysis

Data were analyzed using SPSS software v22.0 (IBM, New York, USA). Inter-reader agreement in detecting saccular hydrops on both methods was estimated using Cohen's kappa coefficient. The concordance between the three sequences was evaluated using the Cohen's kappa coefficient. We considered a k value greater than 0.80 as very good agreement and less than 0.2 as very poor agreement¹⁷. Continuous data are presented as mean and

standard deviation. The rate of SURI with delayed 3D-FLAIR sequence and saccular hydrops with FIESTA-C sequence in MD patients was estimated by the exact Clopper-Pearson interval. The Brunner-Munzel test was used to explore the correlation between the presence of the SURI and saccular hydrops and the degree of hearing loss. Sensitivity and specificity were estimated by taking the clinical examination as the gold standard.

Categorical data are reported as frequency and percentages. We set the significance threshold (p-values) at 0.05.

Results:

Population

Thirty patients were included (19 women) with a mean age of 55.6 [41.6; 69.6] years. Patients referred with unilateral MD, 12 on the right and 18 on the left were confirmed with AAO-HNS criteria. The mean hearing loss was evaluated as being 41.8 +/- 30.2 dB. There were 15 patients with a hearing loss < 40 dB (11 patients with no hearing loss at the time of MRI, 4 patients with mild hearing loss) and 15 patients with a hearing loss > 40 dB (8 patients with moderate hearing loss, 5 with severe hearing loss and 2 patients with profound hearing loss).

MRI data

On delayed post-contrast 3D-FLAIR sequence, 15 patients out of 30 (50%, IC95: 32.5% ; 67.5%) referred with a SURI sign. The right ear was involved in

7 patients and the left ear in 8 patients. This morphological sign was never seen on the contralateral side as the clinical disease (0%, IC95: 0% ; 9.5%). The mean hearing loss was 59.6 +/- 30.1 dB when a SURI sign was present while it was 24 +/- 17.6 dB without a SURI sign. There was a correlation between the degree of hearing loss and the presence of a SURI sign on the Brunner-Munzel test (0.85, IC95: 0.65 ; 0.95). A SURI sign was present in 13/15 patients (86.6%, OR=34.1%, IC95: 4.9 ; 383.6) with hearing loss >40dB and present in 2 patients (18%) with hearing threshold below 40 dB.

The specificity and the sensitivity to detect MD side were 100% and 50% respectively. The inter-rater agreement was 0.87 on the symptomatic and the asymptomatic ears (60 ears) for SURI evaluation with 4 cases of discordance.

On non-enhanced 3D FIESTA-C sequence, 16 patients out of 30 (53.3%) referred with a saccular hydrops. The right ear was involved in 11 patients and the left ear in 5 patients. This morphological sign was seen in 10 patients out of 30 (33.3%, IC95: 18.3% ; 51.4%) to the same side as the clinical disease. A saccular hydrops was seen in 6 patients on the clinical asymptomatic ear (23.3%, IC95: 10.8% ; 40.8%). The mean hearing loss was 45.1 +/- 32.9 dB when a saccular hydrops was present while it was 40.1 +/- 29.6 dB without a saccular hydrops. A saccular hydrops was observed in 4/15 patients (26.6%, OR=1, IC95: 0.21 ; 4.9) with hearing loss >40 dB and in 6 patients (54.5%) with hearing threshold below 40 dB.

The specificity and the sensitivity to detect MD side were 80% and 33.3% respectively. The inter-rater agreement was 0.7 for saccular hydrops on the symptomatic and the asymptomatic ears (60 ears) with 8 cases of discordance.

On delayed 3D FIESTA-C sequence, 13 patients out of 30 (43.3%) referred with a saccular hydrops. The right ear was involved in 11 patients and the left ear in 5 patients. This morphological sign was seen in 8 patients out of 30 (26.6%, IC95: 13.2% ; 44.4%) to the same side as the clinical disease. A saccular hydrops was seen 4 patients on the controlateral side as the clinical disease (16.7%, IC95: 6.4% ; 33.1%). The mean hearing loss was 45.3+/-37 dB when a saccular hydrops was present while it was 40.5+/-28.3 dB without a saccular hydrops. A saccular hydrops was observed in 4/15 patients (26.6%, OR=1, IC95: 0.21 ; 4.9) with hearing loss >40dB and in 4 patients (36.3%) with hearing threshold below 40 dB.

The specificity and the sensitivity to detect MD side were 83.3% and 26.6% respectively. The inter-rater agreement was 0.61 on the symptomatic and the asymptomatic ears (60 ears) for saccular hydrops with 8 cases of discordance.

The concordance between 3D-FLAIR and non-enhanced (Kappa=0, IC95: -0.34 ; 0.35) and post-contrast delayed 3D FIESTA-C sequences (Kappa=0, IC95: -0.23 ; 0.49) was very poor. Among the 15 patients with a SURI sign, 6 patients and 4 patients also presented a saccular hydrops on the non-enhanced 3D FIESTA-C and delayed 3D FIESTA-C sequences respectively.

The concordance between the non-enhanced 3D FIESTA-C and the delayed post-contrast 3D FIESTA-C was good (Kappa=0.68, IC95: 0.40 ; 0.97). Among the 10 patients with a saccular hydrops to the same side as the clinical disease on non-enhanced 3D FIESTA-C, 7 patients also have a saccular

hydrops on the delayed 3D FIESTA-C but 3 patients had a normal saccule on the same sequence and also on delayed 3D-FLAIR.

Among the 8 patients with a saccular hydrops to the same side as the clinical disease on delayed 3D FIESTA-C, 7 patients presented a saccular hydrops on non-enhanced 3D FIESTA-C sequence.

Discussion

We demonstrated that the concordance between 3D-FLAIR and non-enhanced and post-contrast delayed 3D FIESTA-C sequences was very poor. We also showed that the SURI sign as evaluated by the delayed post-contrast 3D-FLAIR enables the diagnosis of saccular hydrops in 50% of cases with a very good inter-reader agreement and it is highly specific of the side of MD symptoms. By contrast, saccular hydrops as evaluated by non-enhanced and delayed 3D FIESTA-C sequences is found in only 33% and 23% of cases respectively with a poorer inter-reader agreement and specificity.

Among the 15 patients with a SURI sign, 6 patients and 4 patients also presented a saccular hydrops on the non-enhanced 3D FIESTA-C and delayed 3D FIESTA-C sequences respectively. To explain this discordance between the delayed 3D-FLAIR and 3D FIESTA-C sequences we based our hypothesis on histological studies. EH involves the cochlear duct in all cases, the saccule in 80% of cases, the utricle and ampullas less constantly¹⁸. Rauch et al. have also described saccular involvement in almost all cases and its distension appeared correlated to the degree of membranous distortion towards the footplate¹⁹. Frequently, the cecum vestibular of the cochlear duct

extends into the vestibule, thus the cecum vestibular and the distended saccule are competing to occupy the vestibule ²⁰. The distension of one of these two structures causes the collapse of the second. We raised the hypothesis that in case of vestibular cecum distension, the inferior part of the vestibule appears in low-signal with delayed 3D-FLAIR sequence while the saccule wall appears normal with 3D FIESTA-C.

Three patients had a normal saccule on delayed 3D FIESTA-C and 3D-FLAIR sequences while a saccular hydrops was observed on non-enhanced 3D FIESTA-C as the same side as the clinical disease. Since 3D FIESTA-C is sensitive to gadolinium, we have speculated that the perilymphatic enhancement allowed a clear discrimination of the boundaries of the saccule.

How to evaluate EH in MD patients: delayed post-contrast 3D-FLAIR or non-enhanced 3D-FIESTA-C?

3D-FLAIR sequences with variable flip angle refocusing have the advantage of increasing echo train length enabling a shorter acquisition time without blurring and of being more sensitive than conventional 3D-FLAIR sequences to detect T1-shortening ^{21,22}. The blood-labyrinthin barrier allows the passage of various structures including gadolinium in the perilymphatic space only but not in the endolymphatic space due to the presence of tight junctions ^{7,8,15}. Using the semi-quantitative method described by Nakashima et al., the rate of EH ranges from 47% to around 90% ²³⁻²⁵. Case-controlled imaging studies demonstrated that the semi-quantitative method was not specific of MD and

depends on the Time Inversion that could modify the endolymph to perilymph ratio ^{2,10}. An anatomic grading system was then proposed, based on the saccular-morphology using the SURI sign with the utricle as an anatomical landmark owing to its low mechanical compliance ⁸⁻¹¹. The SURI sign allows the diagnosis of EH in 50% in a subset of MD patients with 100% specificity. Moreover, saccular hydrops was highly correlated with MD patients with hearing level above 40 dB ¹¹.

The 3D FIESTA-C is a steady-state free precession (SSFP) sequence and a refocused steady-state gradient echo sequence that provides high signals from tissues with elevated T2/T1 ratios and an excellent spatial resolution. The contrast is based on T2/T1 ratios ²⁶. Here, we assess the saccule in MD patients with a high spatial resolution and with a much more reasonable acquisition time (4 minutes 40 seconds) than 3D-FLAIR sequences where the time scans could be up to 15 minutes ²⁷. However, our results (sensitivity 33% and specificity 80%) differ from Venkatasamy et al. and Simon et al. that found a sensitivity of 84% and 63% respectively ^{12,13}. One can explain this difference by the fact that in our study we have included patients with possible, probable and definite MD while Venkatasamy et al. have only included patients with definite MD. In addition, 16% of our patients presented SH on the contralateral asymptomatic clinical ear, which was not precise in the study of Venkatasamy et al. As Venkatasamy et al., our imaging examination was carried out on a 3T General Electric Discovery® MRI scanner. The parameters of the 3D FIESTA-C sequence were closely similar except that we employed the ARC parallel imaging technique reducing acquisition time allowing to reduce motion artifact

and without decreasing significantly the signal-to-noise ratio (SNR). We also used a surface coil allowing to reduce the FOV with minimization of wrap artifacts and to improve SNR and spatial resolution ²⁸.

We could mention that 3D FIESTA-C sequences allow the evaluation of the saccular morphology only which is crucial for the diagnosis of the SH. However, it has been reported recently that patients with vestibular symptoms could show an impairment of the utricle only ²⁹. Furthermore, delayed 3D-FLAIR sequences also enable the assessment of the blood-labyrinthine permeability that can be impaired in other vestibular disorders, such as vestibular neuritis ³⁰⁻³³.

Therapeutic implications

An invasive procedure concerns MD patients with intractable vertigo in almost 30% of cases ³⁴. Two surgical procedures have been widely discussed with variable results on vertigo symptoms: the endolymphatic sac surgery and vestibular neurectomy ^{35,36}. Intratympanic administration of gentamycin enables the control of vertigo in most cases by damaging the sensory hair cells ^{37,38}. Here, we demonstrated that some patients with MD symptoms presented without MRI evidence of saccular hydrops. In MD patients, the invasive treatment could be further discussed with regards to results of the MRI hydrops protocol.

Limitations of this study

The main problem we encountered was the impossibility of confirming the presence of EH with pathological analysis *in vivo*. Further multicenter studies are needed in a larger population to assess the feasibility of T2-weighted echo-gradient sequences with other manufacturers such as Philips® (Balance Fast Field Echo sequence = bFFE) and Siemens® (Constructive Interference in Steady State sequence = CISS).

The height and width of the saccule could not be measured on delayed 3D-FLAIR since some patients with saccular hydrops present a low-signal of the entire lower part of the vestibule making difficult the distinction between the dilated endolymphatic space and the surrounding bone. Moreover, it has been reported that the volume of the endolymphatic depends on the inversion time¹⁰.

In this study, the cochlear endolymphatic compartment was not assessed since it has been reported that healthy subjects could display cochlear duct dilatation, and that it is not visible on T2-weighted sequences, such as the utricle⁸. Furthermore, we decided to compare two grading systems based on the saccular morphology.

Conclusion

Delayed post-contrast 3D-FLAIR enables the diagnosis of EH with a very good inter-reader agreement and it is highly specific of MD symptoms. By contrast,

3D FIESTA-C sequences are less sensitive and specific and allow the diagnosis of EH with a poorer inter-reader agreement.

Acknowledgments:

We are grateful to Nikki Sabourin-Gibbs for editing the manuscript.

References

1. Altman F, Fowler E. Histological findings of Meniere's syndrome complex. *Ann Otol Rhinol Laryngol* 1943 ;52:52-80.
2. Lopez-Escamez J, Attyé A. Systematic review of magnetic resonance imaging for diagnosis of Meniere disease. *J Vestibul Res Equil* 2018 (In press)
3. Naganawa S, Yamazaki M, Kawai H, Bokura K, Sone M, Nakashima T. Visualization of endolymphatic hydrops in Ménière's disease with single-dose intravenous gadolinium-based contrast media using heavily T2-weighted 3D-FLAIR. *Magn Reson Med Sci* 2010;9(4):237–242.
4. Naganawa S, Yamazaki M, Kawai H et al. Visualization of endolymphatic hydrops in Ménière's disease after single-dose intravenous gadolinium-based contrast medium: timing of optimal enhancement. *Magn Reson Med Sci* 2012;11:43–51
5. Niyazov DM, Andrews JC, Strelhoff D, Sinha S, Lufkin R. Diagnosis of endolymphatic hydrops in vivo with magnetic resonance imaging. *Otol Neurotol* 2001;22:813-817.
6. Jahnke K. The blood-perilymph barrier. *Arch Otorhinolaryngol* 1980;228:29—34.
7. Pender DJ. Membrane Stress in the Human Labyrinth and Meniere Disease: A Model Analysis. *Int Arch Otorhinolaryngol*. 2015;19(4):336–342.
8. Attyé A, Eliezer M, Boudiaf N, et al. MRI of endolymphatic hydrops in patients with Meniere's disease: a case-controlled study with a simplified classification based on saccular morphology. *Eur Radiol* <https://doi.org/10.1007/s00330-016-4701-z>.

9. Attyé A, Eliezer M, Galloux A, Pietras J, Tropres I, Schmerber S, et al. Endolymphatic hydrops imaging: Differential diagnosis in patients with Meniere disease symptoms. *Diagn Interv Imaging*. 2017 Oct;98(10):699–706.
10. Eliezer M, Gillibert A, Tropres I, Krainik A, Attyé A. Influence of inversion time on endolymphatic hydrops evaluation in 3D-FLAIR imaging. *J Neuroradiol* 2017 Sep;44(5):339–43.
11. Attyé A, Eliezer M, Medici M, Tropres I, Dumas G, Krainik A, et al. In vivo imaging of saccular hydrops in humans reflects sensorineural hearing loss rather than Meniere's disease symptoms. *Eur Radiol* 2018 Jul;28(7):2916–22.12.
12. Simon F, Guichard JP, Kania R, Franc J, Herman P, Hautefort C. Saccular measurements in routine MRI can predict hydrops in Menière's disease. *Eur Arch otorhinolaryngol* 2017 DOI 10.1007/s00405-017-4756-8
13. Venkatasamy A, Veillon F, Fleury A, Eliezer M, Abu Eid M, Romain B, Vuong H, Rohmer D, Charpiot A, Sick H, Riehm S. Imaging of the saccule for the diagnosis of endolymphatic hydrops in Meniere disease, using a three-dimensional T2-weighted steady state free precession sequence: accurate, fast, and without contrast material intravenous injection. *Eur Radiol Exp* 2017; 1:14 DOI 10.1186/s41747-017-0020-7
14. Committee on Hearing and Equilibrium guidelines for the diagnosis and evaluation of therapy in Menière's disease. American Academy of Otolaryngology-Head and Neck Foundation, Inc. *Otolaryngol--Head Neck Surg Off J Am Acad Otolaryngol-Head Neck Surg*. 1995;113(3):181-185.
15. Eliezer M, Poillon G, Gillibert A, Horion J, Cruyppeninck Y, Gerardin E, et al. Comparison of enhancement of the vestibular perilymph between gadoterate

- meglumine and gadobutrol at 3-Tesla in Meniere's disease. *Diagn Interv Imaging*. 2018 May;99(5):271–7.
16. Veillon F, Ramos-Taboada L, Abu-Eid M, Charpiot A, Riehm S. Imaging of the facial nerve. *Eur J Radiol* 2010;74:341-348.
 17. Portney LG, Watkins MP. *Foundations of clinical research: applications to practice*. New Jersey: Prentice Hall; 2000.
 18. Pender DJ. Endolymphatic hydrops and Ménière's disease: a lesion meta-analysis. *J Laryngol Otol*. 2014; 128(10):859–865.
 19. Rauch SD, Merchant SN, Thedinger BA. Meniere's syndrome and endolymphatic hydrops. Double-blind temporal bone study. *Ann Otol Rhinol Laryngol* 1989;98:873-883.
 20. Merchant S, Nadol J (eds) (2010) *Schuknecht's pathology of the ear*, 3rd edn. McGraw-Hill Education (UK), London, ISBN 978 1 60795 030 1
 21. Mugler JP, Bao S, Mulkern RV, Guttmann CR, Robertson RL, Jolesz FA, Brookeman JR. Optimized single-slab three-dimensional spin-echo MR imaging of the brain. *Radiology* 2000; 216:891–899
 22. Naganawa S. The technical and clinical features of 3D-FLAIR in neuroimaging. *Magn Reson Med Sci MRMS Off J Jpn Soc Magn Reson Med*. 2015; 14(2):93–106.
 23. Nakashima T, Naganawa S, Pyykkö I, et al. Grading of endolymphatic hydrops using magnetic resonance imaging. *Acta Oto-Laryngol Suppl* 2009. doi: 10.1080/00016480902729827
 24. Baráth K, Schuknecht B, Monge Naldi A et al. Detection and grading of endolymphatic hydrops in Meniere disease using MR imaging. *AJNR Am J Neuroradiol* 2014. doi:[10.3174/ajnr.A3856](https://doi.org/10.3174/ajnr.A3856)□6.

25. Pyykkö I, Nakashima T, Yoshida T et al. Meniere's disease: a reappraisal supported by a variable latency of symptoms and the MRI visualisation of endolymphatic hydrops. *BMJ Open* 2013. doi:[10.1136/bmjopen-2012-001555](https://doi.org/10.1136/bmjopen-2012-001555)7.
26. Chavhan GB, Bobby PS, Jankharia BG, Cheng HLM, Shroff MM. Steady-state MR imaging sequences: physics, classification, and clinical applications. *Radiographics* 2008;28(4):1147-60. doi: 10.1148/rg.284075031.
27. Hagiwara M, Roland JT, Wu X, Nusbaum A, Babb JS, Roehm PC, et al. Identification of endolymphatic hydrops in Ménière's disease utilizing delayed postcontrast 3D Flair and fused 3D Flair and CISS color maps. *Otol Neurotol* 2014;35:e337–42, <http://dx.doi.org/10.1097/MAO.0000000000000585>.
28. Bykowski J, Harris JP, Miller M, Du J, Mafee MF. Intratympanic contrast in the evaluation of Ménière disease: understanding the limits. *AJNR Am J Neuroradiol* 2015;36(7):1326-1332.
29. Eliezer M, Attyé A, Guichard JP, Vitaux H, Guillonnet A, Toupet M, Herman P, Kania R, Houdart E, Hautefort C. Vestibular atelectasis: myth or reality? *Laryngoscope* 2019 doi:[10.1002/lary.27793](https://doi.org/10.1002/lary.27793).
30. Tagaya M, Yamazaki M, Teranishi M, Naganawa S, Yoshida T, Otake H, et al. Endolymphatic hydrops and blood-labyrinth barrier in Ménière's disease. *Acta Otolaryngol (Stockh)*. 2011 May;131(5):474–9.
31. Pakdaman MN, Ishiyama G, Ishiyama A, Peng KA, Kim HJ, Pope WB, et al. Blood-Labyrinth Barrier Permeability in Ménière Disease and Idiopathic Sudden Sensorineural Hearing Loss: Findings on Delayed Postcontrast 3D-FLAIR MRI. *AJNR Am J Neuroradiol*. 2016 Oct;37(10):1903–8.

32. Naganawa S, Kawai H, Taoka T, Suzuki K, Iwano S, Satake H, et al. Cochlear Lymph Fluid Signal Increase in Patients with Otosclerosis after Intravenous Administration of Gadodiamide. *Magn Reson Med Sci MRMS Off J Jpn Soc Magn Reson Med*. 2016 Jul 11;15(3):308–15.
33. Eliezer M, Maquet C, horion J, Gillibert A, Toupet M, Bolognini B, Magne N, Kahn Laureline, Hautefort C, Attyé A. detection of intralabyrinthine abnormalities using post-contrast delayed 3D-FLAIR sequences in patients with acute vestibular syndrome. *Eur Radiol* 2018 <https://doi.org/10.1007/s00330-018-5825-0>
34. Sajjadi H, Paparella MM. Meniere's disease. *Lancet*. 2008; 372(9636):406–414.
35. Paparella MM. Endolymphatic sac revision for recurrent intractable Meniere's disease. *Otolaryngol Clin North Am*. 2006;39(4):713–721, vi.
36. Kitahara T, Fukushima M, Uno A, et al. Long-term results of endolymphatic sac drainage with local steroids for intractable Meniere's disease. *Auris Nasus Larynx*. 2013;40(5):425–430.
37. Miller MW, Agrawal Y. Intratympanic Therapies for Menière's disease. *Curr Otorhinolaryngol Rep*. 2014;2(3):137–143.
38. Cohen-Kerem R, Kisilevsky V, Einarson TR, Kozler E, Koren G, Rutka JA. Intratympanic gentamicin for Menière's disease: a meta-analysis. *Laryngoscope* 2004;114:2085–2091.

Figure 1

(A) Coronal non-enhanced 3D FIESTA-C sequence at the level of the superior (gray arrow) and lateral semicircular canals (dotted gray arrow) showing a normal saccule (white arrow) below the utricular macula (white dotted arrow).

The sagittal reference slice (D) allowing to apply the SURI method was obtained using multiplanar reconstructions with the axial (B) and coronal (C) slices passing through the utricle (gray arrow) and the saccule (white arrow).

Figure 2

70 year-old female with a left MD

(B) Coronal non-enhanced 3D FIESTA-C sequence at the level of the superior (gray arrow) and lateral semicircular canals (dotted gray arrow) showing a normal saccule (white arrow; height: 1.6 mm; width: 1.3 mm) below the utricular macula (white dotted arrow).

(C) Coronal delayed 3D FIESTA-C sequence at the level of the superior (gray arrow) and lateral semicircular canals (dotted gray arrow) showing a normal saccule (white arrow; height: 1.6 mm; width: 1.3 mm) below the utricular macula (white dotted arrow).

(D) Axial 3D-FLAIR at the level of the saccule (white arrow) and the posterior ampulla (white dotted arrow) demonstrating a left saccular hydrops.

Figure 3

48 year-old male with a left MD

(A) Coronal non-enhanced 3D FIESTA-C sequence at the level of the superior (gray arrow) and lateral semicircular canals (dotted gray arrow) showing a left saccular hydrops (white arrow; height: 2.5 mm; width: 1.5 mm) below the utricular macula (white dotted arrow).

(B) Coronal delayed 3D FIESTA-C sequence at the level of the superior (gray arrow) and lateral semicircular canals (dotted gray arrow) showing a left saccular hydrops (white arrow; height: 2.5 mm; width: 1.5 mm) below the utricular macula (white dotted arrow).

(C) Axial 3D-FLAIR at the level of the saccule (gray dotted arrow) and posterior ampulla (white dotted arrow) demonstrating a left saccular hydrops.

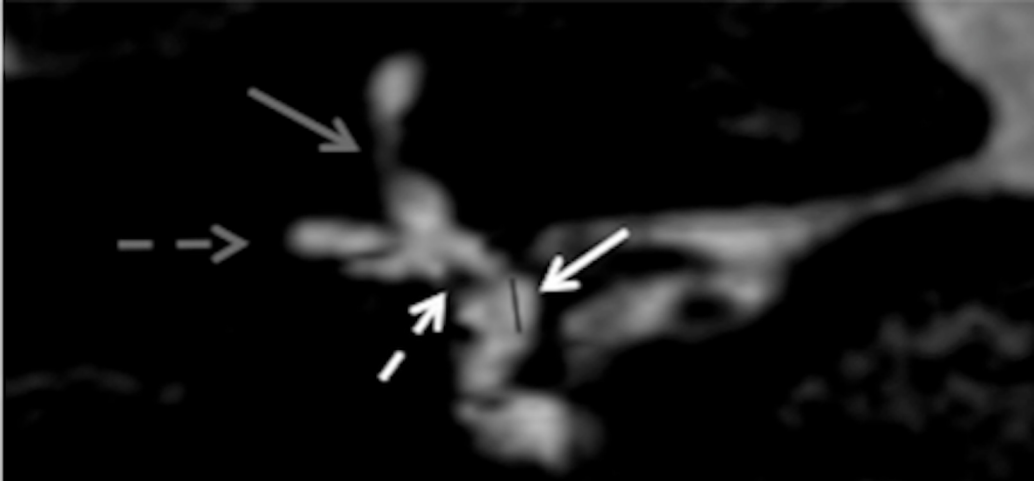
Figure 4

47 year-old female with a left MD

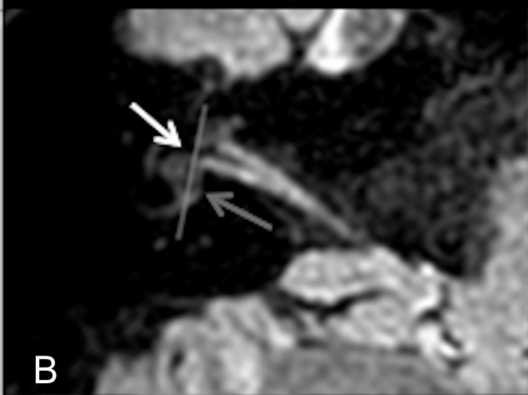
(A) Coronal non-enhanced 3D FIESTA-C sequence at the level of the superior (gray arrow) and lateral semicircular canals (dotted gray arrow) showing a left saccular hydrops (white arrow; height: 2.1 mm; width: 1.1 mm) below the utricular macula (white dotted arrow).

(B) Coronal delayed 3D FIESTA-C sequence at the level of the superior (gray arrow) and lateral semicircular canals (dotted gray arrow) showing a left normal saccule (white arrow; height: 1.5 mm; width: 1.3 mm) below the utricular macula (white dotted arrow).

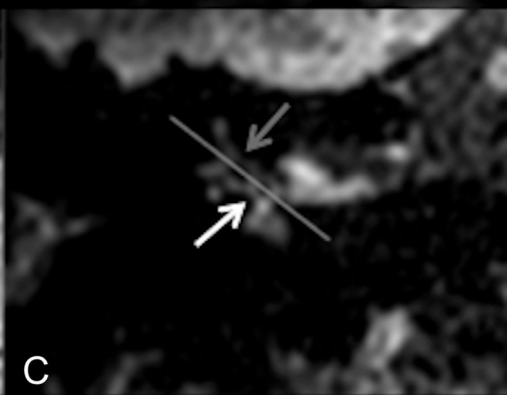
(C) Axial 3D-FLAIR at the level of the saccule (gray dotted arrow) and lower part of the utricle (white dotted arrow) demonstrating a left normal saccule.



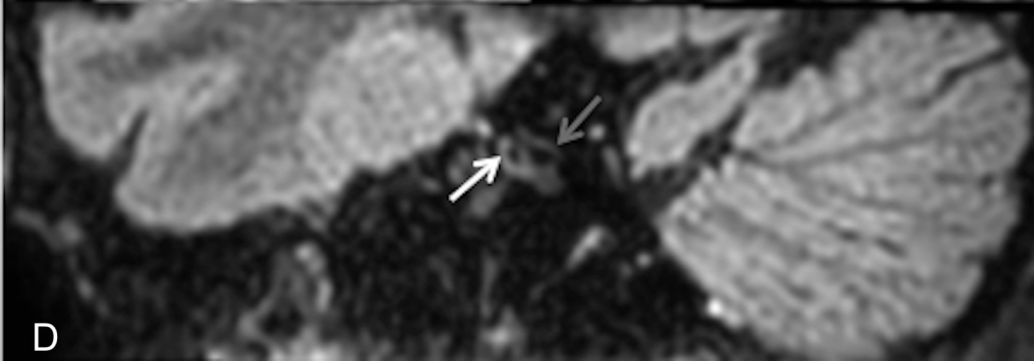
A



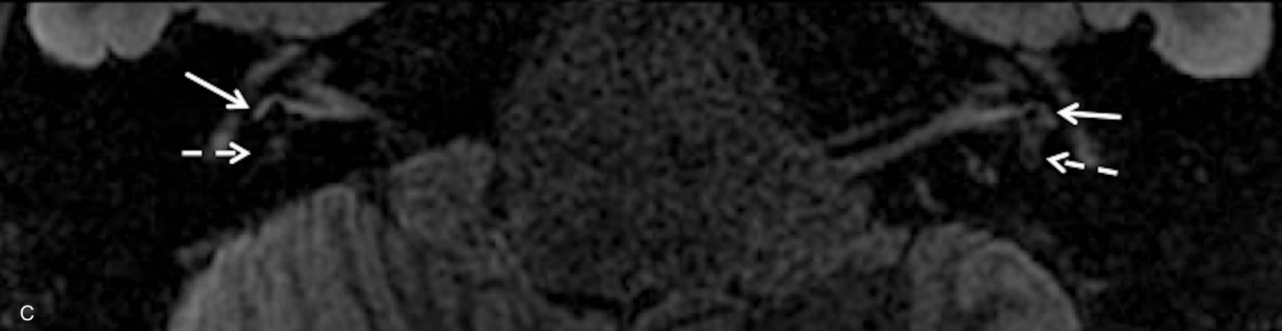
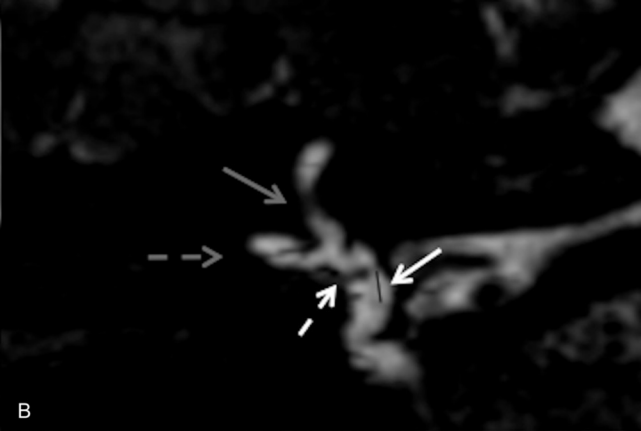
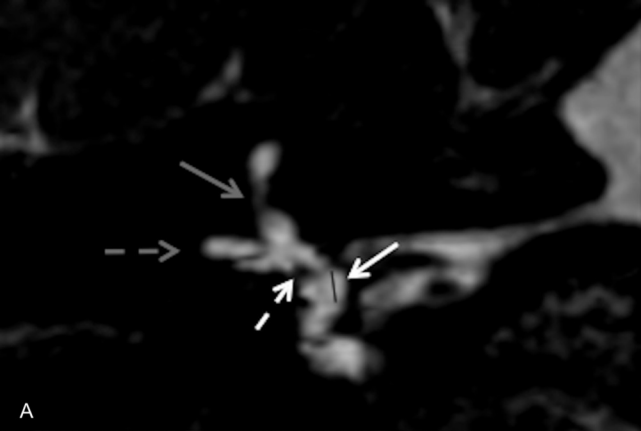
B

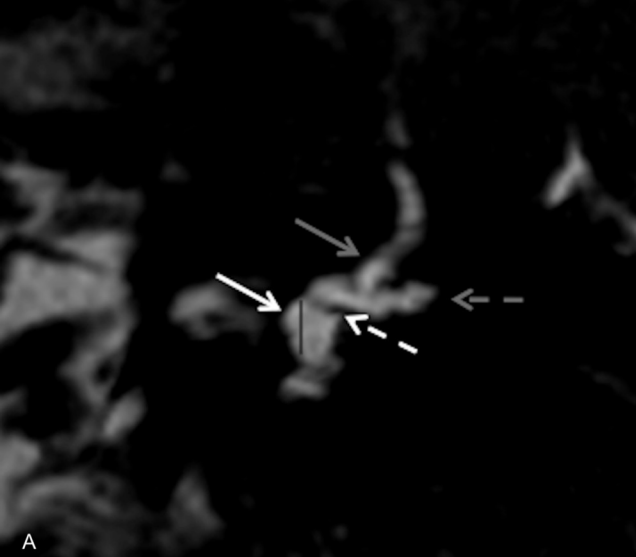


C

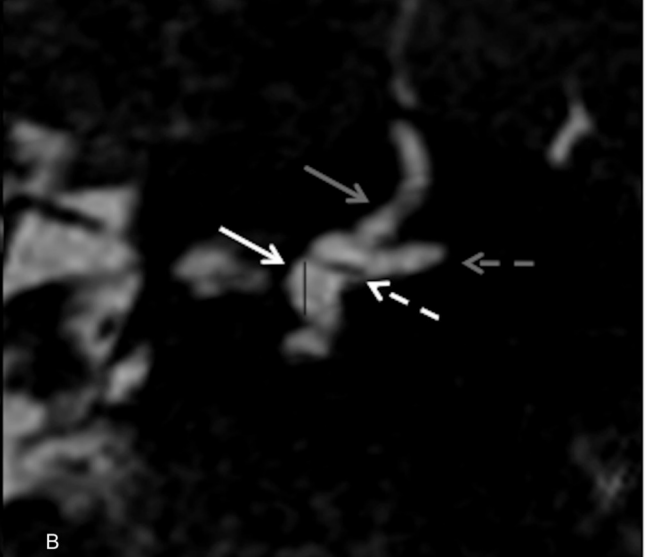


D





A



B



C

